An inversion procedure for coupled-channel scattering: determining the deuteron-nucleus tensor interaction.

S.G. Cooper[†], V.I. Kukulin[‡], R.S. Mackintosh[†] and V.N. Pomerantsev[‡]

[†]*Physics Department, The Open University, Milton Keynes, MK7 6AA, U.K.*

[‡]*Institute of Nuclear Physics, Moscow State University, Moscow 119899, Russia.*

(February 9, 2008)

Abstract

We present a practical S-matrix to potential inversion procedure for coupled-channel scattering. The inversion technique developed is applied to non-diagonal $S^J_{ll'}$ for spin one projectiles, yielding a tensor interaction T_R and is also applicable to spin-$\frac{1}{2}$ plus spin-$\frac{1}{2}$ scattering. The method is a generalization of the iterative-perturbative, IP, method. It is tested and evaluated and we investigate the degree of uniqueness of the potential, particularly for cases where there is insufficient information to define the potential uniquely. We examine the potentials which result when the S-matrix is generated from a T_P interaction. We also develop the generalisation, using established procedures, of IP S-matrix-to-potential inversion to direct observable-to-potential inversion. This 'direct inversion' procedure is demonstrated to be an efficient method for finding a multi-component potential including a T_R interaction fitting multi-energy σ, iT_{11}, T_{20}, T_{21} and T_{22} data for the scattering of spin-1 nuclei from spin-zero target. It is applicable to other channel spin 1 cases.

PACS numbers: 21.30.-x, 13.75.Cs, 25.10.+s

Typeset using REVTEX

I. INTRODUCTION

Various methods for carrying out S-matrix to potential inversion are now available, see for example [1,2], but, until recently, it has been possible only for cases with channel-spin zero or 1/2. However, there have been many accurate experiments involving spin-one polarised particles and these provide a powerful motivation to develop an efficient technique for inversion in cases with higher channel spin, i.e. coupled-channel scattering. With such a technique, one can exploit the very large volume of polarisation data which has accumulated. This includes vector and tensor analysing powers and polarisation transfer observables.

Over the years, we have developed a practical and widely generalisable procedure, the iterative perturbative, IP, method [3–7] and we recently [8] demonstrated an extension to spin-1 projectiles for the first time. Ref. [8] demonstrates the method in one specific application, but does not give details or a derivation of the method. In this paper we present details of our extension of the IP S-matrix to potential inversion method to the coupled-channel case of spin-1 projectiles and present further evaluation of it. We also test and evaluate an important extension of the IP method, single step data-to-potential inversion for coupled-channel scattering.

In Ref. [8] we applied single step inversion to analyse real data. We note here that there are also many ways in which IP $S \rightarrow V$ inversion can contribute to understanding nucleus-nucleus interactions. Perhaps the most obvious application is the inversion of S-matrix elements found by phase shift analysis of experimental data. However, there are also many important applications which involve the inversion of theoretical S-matrix elements, i.e. elastic channel S derived from coupled channel calculations, Glauber model and resonating group model calculations. The potential found in this way contains information concerning the contribution of tensor components to dynamic polarization and exchange processes to inter-nuclear potentials. For the particular case of spin-polarised deuteron and ^{6}Li scattering, obvious applications include the study of the influence of reaction channels and distortion effects on the projectile-nucleus potential, especially in its non-central components. There are a number of longstanding puzzles relating to spin-polarised deuteron scattering, including the anomalously small real part of the tensor interaction, which can be studied using these methods.

Coupled-channel inversion represents a significant development in inversion techniques since a non-diagonal potential is derived from a non-diagonal S-matrix. Such a potential couples channels of the same conserved quantum numbers but different values of orbital angular momentum. Spin-1 inversion is therefore the first example of coupled channel inversion in which a non-diagonal S-matrix is made to yield a non-diagonal potential. Apart from the general derivation, the present paper is framed for a very specific two-channel case: deuterons scattering from a spin zero nucleus with inversion determining a tensor interaction involving the non-diagonal operator T_R as given below. In spite of the rather specific nature of the present application, we believe this work opens the way to a fully general class of coupled-channel inversion situations involving the determination of a coupling potential from a non-diagonal S-matrix.

This paper presents in detail only those aspects of the IP inversion formalism which are connected with the specific coupled channel generalisation to spin-1 scattering. In other respects it calls upon previous publications [5–7] in which the general aspects of the IP

inversion procedure are described. Because of the specific application to spin-1 projectiles, we establish our notation by beginning in Section II with a brief review of basic aspects of spin-1 scattering.

An important feature of the IP $S \rightarrow V$ inversion procedure is the natural way in which it can be convoluted with (data) $\rightarrow S$ fitting to give an overall (data) $\rightarrow V$ algorithm. This provides a new and efficient data analysis tool which in many cases obviates the need for independent (data) $\rightarrow S$ inversion. Important advantages follow when fitting data for many energies since the underlying potential model guarantees that the energy dependence of the S-matrix will be smooth without the need to postulate parameterized forms for $S(E)$. Indeed, we have shown [9] that (data) $\rightarrow V$ inversion can provide a powerful alternative method for phase shift fitting of multi-energy scattering data for light nuclei.

Ref. [8] contained a restricted analysis of low energy $\vec{d}$ + ^{4}He data. A future paper will present a much more exhaustive analysis of the very large collection of data for this system. At a later stage we hope to present an analysis of $^6\vec{\text{Li}}+^4$He data, including tensor analysing powers.

II. THE SCATTERING OF SPIN-1 NUCLEI FROM SPIN-0 TARGETS

A. Formalism for spin-1 scattering

In order to establish our notation, we outline the standard formalism for the elastic scattering of spin-1 projectiles from a spin-0 target in the presence of tensor forces. The key feature introduced by the tensor interaction of T_{R} type (see below for a classification of tensor forces) is that it couples channels of different orbital angular momentum l. Specifically, for particular values of the conserved quantities J, the total angular momentum, and π, the parity, whenever $\pi = (-1)^{J+1}$, then two values of orbital angular momentum, $l = J-1$ and $J+1$, are coupled by T_{R}.

For total angular momentum J and orbital angular momentum l' the radial wavefunction $\psi_{l'l}^J$ satisfies the coupled equations,

$$\left[\frac{\mathrm{d}^2}{\mathrm{d}r^2} + k^2 - \frac{2\mu}{\hbar^2}(l'J|V|l'J) - \frac{l'(l'+1)}{r^2} \right] \psi_{l'l}^J(k,r) = \sum_{l'' \neq l'} \frac{2\mu}{\hbar^2}(l'J|V|l''J)\psi_{l''l}^J(k,r) \qquad (1)$$

where μ is the reduced mass of the system and $(l'J|V|l''J)$, a function of r, is the matrix element of the inter-nuclear interaction V integrated over all angular and internal degrees of freedom. The second subscript, l, on ψ identifies the incoming orbital angular momentum. This is determined by imposing on the solution of the coupled equations, the following asymptotic boundary conditions :

$$\psi_{l'l}^J(k,r) \rightarrow \delta_{l'l}I_{l'}(kr) - S_{l'l}^J O_{l'}(kr). \qquad (2)$$

Here, $I_l(r)$ and $O_l(r)$ are the incoming and outgoing asymptotic Coulomb radial wavefunctions, often written $H_l(r)^*$ and $H_l(r)$ respectively as in Satchler [10], namely:

$$I_l(kr) = G_l(kr) - \mathrm{i}F_l(kr); \qquad I_l(kr) = G_l(kr) - \mathrm{i}F_l(kr);$$

where F_l and G_l are regular and irregular Coulomb wavefunctions respectively. Note that the boundary conditions given in Eq. 2 differ by a factor from those adopted by Satchler. Where there is no ambiguity, we suppress the J superscript. When $\pi = (-1)^J$, V is diagonal and Eq. 1 is uncoupled.

In general, S will not be unitary, but will be subject to the unitarity limits: $|S_{11}|^2 + |S_{12}|^2 \leq 1$ and $|S_{22}|^2 + |S_{21}|^2 \leq 1$, where, of course $S_{12} = S_{21}$. These limits present no particular problem for $S \to V$ inversion where S can be assumed to satisfy them, but they can represent a significant problem in the case of data to potential inversion, see Section VI.

B. The T_R interaction and its effect.

Non-diagonal matrix elements $(l'J|V|l''J)$ occur in Eqn. 1 for elastic scattering of spin-1 projectiles with certain types of tensor force. The possible forms of local tensor interaction have been classified by Satchler [13,10] who defined T_R, T_L and T_P interactions. The T_L interaction is believed [14] to be very small, at least below 50 MeV/u, and is in any case diagonal in l. The T_P interaction could well be substantial [15] but appears to be hard to distinguish phenomenologically from T_R. The gradient operators within T_P make calculations harder, and the present inversion method does not apply to it.

1. The T_R operator

In this work we assume that the inter-nucleus potential V contains a tensor force component of T_R form [10]:

$$T_R V_R(r) \equiv ((\mathbf{s} \cdot \hat{\mathbf{r}})^2 - 2/3)V_R(r).\tag{3}$$

We quote the matrix elements of the interaction T_R for future reference. The diagonal matrix elements of T_R are:

	$l = J - 1$	$l = J$	$l = J + 1$
$< Jl\|T_R\|Jl >$	$-\frac{1}{3}\frac{J-1}{2J+1}$	$\frac{1}{3}$	$-\frac{1}{3}\frac{J+2}{2J+1}$

and the non-diagonal matrix elements are:

$$< J\, J - 1|T_R|J\, J + 1 >=< J\, J + 1|T_R|J\, J - 1 >= \frac{[J(J+1)]^{1/2}}{2J+1}.\tag{4}$$

2. The radial form of the T_R interaction

The derivation of $V_R(r)$ from the folding model has been discussed at length long ago by Keaton and his colleagues [16–18] and also by Raynal [19]. Within the folding model, the deuteron T_R interaction arises directly from the D-state component. The overall general success of folding models for central and spin-orbit interactions suggests that folding model calculations of $V_R(r)$ should give at least approximately the correct radial form and

4

overall magnitude, but this has not been borne out in the case of T_{R} according to extensive phenomenological studies, e.g. [20–24]. The overall conclusion is that the real part of $V_R(r)$ predicted by the folding model is much too strong for heavy nuclei, of the right order of magnitude for light target nuclei, and actually about three times too strong for a ^{4}He target.[1] These facts, together with a large literature discussing breakup and reaction channel contributions, suggest that we have no generally applicable reliable knowledge of $V_R(r)$. There is reason to doubt even the general arguments, based on folding models, that it should be small in the interior of heavier nuclei, away from the nuclear density gradients in the surface. Such gradients define the angle between the projectile spin $\mathbf{s}$ and the vectorial position $\mathbf{r}$ of the projectile with respect to the nuclear centre, see Eq. 3.

III. $S \to V$ INVERSION FOR SPIN-1 PROJECTILES ON SPIN-0 TARGETS

A. General background of IP inversion

The IP method has been successful for $S_{lj} \to V(r) + \mathbf{l} \cdot \mathbf{s} V_{\mathrm{so}}(r)$ inversion for spin half projectiles, and we now present its generalisation to spin-1 inversion. The only restriction is to a T_{R} tensor interaction. Certain features of the IP method, to our knowledge not shared by other inversion methods, will be of particular importance in the particular systems to which we shall apply spin-1 inversion. These include the ability to find an explicitly energy dependent potential from phase shifts for a range of energies, the ability to handle a range of energies simultaneously and to include Majorana terms for all potential components. For many applications the important property is that mentioned in the introduction, i.e. that IP inversion lends itself to direct observable to potential inversion. This not only avoids the need for independently determined phase shifts (or S-matrix), but actually provides an advantageous method of determining such phase shifts. For a full description of IP inversion as applied in the spin-1/2 case see Refs. [5–7]. The formalism presented in Ref. [7], whereby energy dependent potentials are obtained from multi-energy datasets, can be used with spin-1 inversion as described here, although energy dependence is not actually exploited in the test cases. A brief general account of IP inversion is given in the next section.

B. IP inversion for the coupled channel case; application to spin-1

Our notation must reflect the fact that the outcome of inversion will be a potential with many components. We therefore label each component with an index p which identifies central, spin-orbit or tensor terms, each real or imaginary. The number of components doubles when the potential is parity dependent. (Parity dependence is particularly important for light nuclei at lower energies.)

————

[1]Ref [8] exploits the inversion formalism presented here to give an alternative analysis of d + ^{4}He scattering, a theme elaborated in later papers.

The IP method commences with a 'starting reference potential', SRP, and proceeds by iteratively correcting each component p of the potential:

$$V^{(p)} \rightarrow V^{(p)} + \sum_n \alpha_n^{(p)} v_n^{(p)}(r) \tag{5}$$

where $\alpha_n^{(p)}$ are coefficients to be determined and $v_n^{(p)}(r)$ are the functions comprising the 'inversion basis', (which, if required, can be chosen differently for different p). The amplitudes $\alpha_n^{(p)}$ are determined at each iteration from linear equations, based on an SVD algorithm, which successively reduce the 'phase shift distance' σ defined by:

$$\sigma^2 = \sum |S_k^{\mathrm{t}} - S_k^{\mathrm{c}}|^2. \tag{6}$$

For each partial wave k, S_k^{t} is the 'target' S-matrix and S_k^{c} is for the potential at the current iteration. Here the label k is a single index which identifies the partial wave angular momentum l as well as the energy E_i when multi energy sets of $S_l(E_i)$ are simultaneously inverted. It also includes non-diagonal elements of $S_{ll'}^J$ in the spin-1 case described later.

The linear equations are based on the (usually) very linear response [5,25], ΔS, of the complex S-matrix to small changes ΔV in the potential. The expression for this is well known in the uncoupled case and is very simple:

$$\Delta S_l = \frac{\mathrm{i}m}{\hbar^2 k} \int_0^\infty (\psi_l(r))^2 \Delta V(r) \mathrm{d}r. \tag{7}$$

In Eq.7, the S-matrix S_l is written in terms of the asymptotic form of the regular radial wave function as $\psi_l(r) \rightarrow I_l(r) - S_l O_l(r)$ where I_l and O_l are incoming and outgoing Coulomb wave functions as before. When inverting $S_l(E_k)$ over a series of energies E_k, the energy label E_k is implicit in these equations with index k subsumed with orbital angular momentum l to give an overall channel label. In the case of spin-1/2, the j label is also subsumed in the same way [7]. Linear algebraic equations for local variations of $\alpha_n^{(p)}$ follow from the minimisation of σ^2, [3–5].

We now present the generalized linear response relationship which applies to the non-diagonal S-matrix for spin-1 elastic scattering. The derivation is given in Section III B 1. For any given set of conserved quantum numbers, certain channels will be coupled by the nucleus-nucleus interaction and we use labels $\kappa, \lambda, \mu, \nu$ for these channels. Thus the matrix element of the nucleus-nucleus interaction V between the wavefunctions for channels κ and λ, corresponding to integrating over all coordinates but r, will be written $V_{\kappa\lambda}(r)$. The increment $\Delta S_{\kappa\lambda}$ in the non-diagonal S-matrix which is due to a small perturbation $\Delta V_{\kappa\lambda}(r)$, is

$$\Delta S_{\kappa\lambda} = \frac{\mathrm{i}\mu}{\hbar^2 k} \sum_{\mu\nu} \int_0^\infty \psi_{\mu\kappa}(r) \Delta V_{\mu\nu}(r) \psi_{\nu\lambda} \mathrm{d}r \tag{8}$$

where $\psi_{\nu\kappa}$ is the νth channel (first index) component of that coupled channel solution for the unperturbed non-diagonal potential for which there is in-going flux in channel κ (second index) only. The normalisation is $\psi_{\nu\kappa} \rightarrow \delta_{\kappa\nu} I_{l_\kappa} - S_{\nu\kappa} O_{l_\nu}$ where I_l and O_l are incoming and outgoing Coulomb wavefunctions for orbital angular momentum l; there is no complex conjugation in the integral. Starting from Eq.8, spin-one inversion becomes a straightforward

generalisation of the procedure outlined above and described in Refs. [5–7]. The method is implemented in the code IMAGO [26] where the linearity relations have been exhaustively tested by the gradient method.

A convenient feature of the IP method is that one can judge from the behaviour of σ^2 as the iteration proceeds whether a satisfactory inversion has been achieved. A low value of σ^2 obviously guarantees that a potential closely reproducing the input S_l has been found. Because the IP method is implemented interactively, there is an opportunity to examine the potential for oscillatory features. These might well be spurious and result from over-fitting noisy data. In such a case, one can reduce the basis dimensionality or raise the SVD limit and this generally allows one to achieve a smooth potential, often with only a small increase in σ^2. One must bear in mind that genuine oscillatory features, corresponding to non-locality in an L-independent local potential or to L-dependence of the underlying potential, can be necessary to achieve a precise representation of S_{lj} or $S_{l'l}^J$.

We stress here that, although the context of our discussion is the determination of a tensor interaction from the non-diagonal S-matrix elements describing the scattering of spin-1 projectiles, the range of application is much more general.

1. Derivation of non-diagonal perturbation expression.

We now outline the derivation of Eq.8. The derivation can be applied to the general coupled channel inversion from non-diagonal S-matrix to non-diagonal potential. Our starting point is Eq.1 which we shall write with a simplified notation for two channels. Until the last step in the argument, we shall assume we are using units in which $\hbar^2/2m = 1$.

The radial wavefunctions in channel i with incoming waves in channel λ are written as $\psi_{i\lambda}$ and have asymptotic behaviour at $r \to \infty$:

$$\psi_{i\lambda} \to \delta_{i\lambda}I_\lambda - S_{\lambda i}O_i \tag{9}$$

where for simplicity we write O_i for the outgoing Coulomb wavefunction with orbital angular momentum ℓ appropriate to channel i, and similarly for the ingoing wavefunction I_i. For brevity we omit labels for conserved quantum numbers J and π.

Absorbing the centrifugal interaction within the potential, we can write the coupled equations for the radial wavefunctions appropriate to incoming waves in channel λ as:

$$\psi_{i\lambda}'' = \sum_j (V_{ij} - E\delta_{ij})\psi_{j\lambda}, \qquad i = 1, 2. \tag{10}$$

In the case considered here, V_{ij} with $i \neq j$ arises entirely from the tensor interaction, the matrix V_{ij} being symmetric. Now, denoting by $\bar{\psi}$ the wavefunction arising from a (symmetric) perturbation in the potential $V_{ij} \to V_{ij} + \Delta V_{ij}$, we can write:

$$\bar{\psi}_{i\lambda}'' = \sum_j (V_{ij} + \Delta V_{ij} - E\delta_{ij})\bar{\psi}_{j\lambda}, \qquad i = 1, 2. \tag{11}$$

Multiplying Eq.10 by $\bar{\psi}_{i\mu}$ and Eq.11 by $\psi_{i\mu}$, summing over i and then subtracting the second one from the first one, we get:

$$\sum_i \frac{\mathrm{d}}{\mathrm{d}r}(\psi'_{i\lambda}\bar{\psi}_{i\mu} - \bar{\psi}'_{i\lambda}\psi_{i\mu}) = -\sum_{ij} \psi_{i\mu}\Delta V_{ij}\bar{\psi}_{j\lambda}, \tag{12}$$

as all terms including V_{ij} in the right hand side vanish due to symmetry of V_{ij}.

Integrating Eq.(12) from $r = 0$ to the asymptotic region and using the usual Wronskian relationship $W[I_\ell, O_\ell] = -2ik$, we get:

$$2ik(\bar{S}_{\mu\lambda} - S_{\lambda\mu}) = \sum_{ij} \int_0^\infty \psi_{i\mu}\Delta V_{ij}\bar{\psi}_{j\lambda}\mathrm{d}r. \tag{13}$$

Since the coupled channel equations with a symmetrical potential matrix give a symmetrical S-matrix $S_{\lambda\mu} = S_{\mu\lambda}$, the left hand side of Eq.(13) is equal

$$2ik(\bar{S}_{\mu\lambda} - S_{\mu\lambda}) = 2ik\Delta S_{\mu\lambda} \tag{14}$$

Hence we find, reinstating the $2m/\hbar^2$ factor on the right hand side:

$$\Delta S_{\lambda\mu} = \frac{im}{\hbar^2 k}\sum_{ij}\int_0^\infty \psi_{i\lambda}\Delta V_{ij}\bar{\psi}_{j\mu}\mathrm{d}r. \tag{15}$$

This expression is valid for any symmetrical finite perturbations ΔV_{ij} decreasing at $r \to \infty$ sufficiently rapidly. It is easily extended to any system of coupled-channel equations. For small ΔV_{ij} we make the Born approximation assumption that $\bar{\psi} \sim \psi$ and get:

$$\Delta S_{\lambda\mu} = \frac{im}{\hbar^2 k}\sum_{ij}\int_0^\infty \psi_{i\lambda}\Delta V_{ij}\psi_{j\mu}\mathrm{d}r. \tag{16}$$

The expression (16) is the basis for the coupled-channel inversion method. The success of the inversion method in leading to a converged solution confirms the wide applicability of this equation in each step of our iteration process.

IV. TESTING COUPLE-CHANNEL $S \to V$ INVERSION FOR SPIN-1 PROJECTILES

We carried out two contrasting tests of $S \to V$ inversion as described in Sections IV B and IV C below. First let us define the potentials and the inversion basis.

A. Specification of the interaction potential and basis used

In one respect our notation is non-standard. We write down the complete potential for spin-1 projectiles scattering from a spin-zero target. It is

$$V_{\mathrm{cen}}(r) + iW_{\mathrm{cen}}(r) + V_{\mathrm{coul}}(r) + 2\mathbf{l}\cdot\mathbf{s}(V_{\mathrm{so}} + iW_{\mathrm{so}}) + (V_{\mathrm{R}} + iW_{\mathrm{R}})T_{\mathrm{R}} \tag{17}$$

where $V_{\mathrm{coul}}(r)$ is the usual hard-sphere Coulomb potential. Note that our spin-orbit potentials V_{so} and W_{so}, are defined in such a way that they will be half the magnitude of those

defined according to the usual convention [10] for spin-1 projectile.[2] For the test cases we present, the spin-orbit potential is defined as in Eq. 17.

For notational simplicity, Eq. 17 has not been written to reflect parity dependence. There are two alternative methods of representing parity dependence. The code IMAGO can apply either of these to each of the components in Eq. 17 except V_{coul}. The first representation defines Wigner and Majorana components for each term, say V_x:

$$V_x = V_{x,W} + (-1)^l V_{x,M} \qquad (18)$$

where l is the partial wave angular momentum. With this form the inversion procedure can be made to determine $V_{x,W}$ and $V_{x,M}$ for any or all V_x. An alternative approach is to determine independent positive or negative parity components for V_x. In many cases, the Wigner-Majorana representation is most natural and has been shown [11] to be preferable where the odd parity term may otherwise be ill-determined. However, sometimes the odd-even representation is more appropriate, for example where a particular V_x has completely different shapes and magnitudes for the different parities, as we believe can be the case for V_R. The code IMAGO offers the freedom to represent the parity dependence of each component V_x in either way.

The IP method is not tied to any particular set of functions for the inversion basis and each component of the potential can be represented by a different basis. It is an important feature of the IP method, as implemented in IMAGO, that a range of different functions is available, and those which we have applied are specified in [26]. Zeroth order Bessel functions and harmonic oscillator functions are both linearly independent sets which have proven useful where bases of large dimensionality are necessary to describe a potential over a wide radial range down to $r = 0$. For cases involving light nuclei, particularly for inversion of small S-matrix datasets, a small basis comprising a series of Gaussian functions is preferable. A Gaussian basis covering just the nuclear surface region is also useful for heavy ion cases where there is no information available to determine the potential in the nuclear interior. It is important that a basis should not be chosen which would describe the potential over a radial range, or to a degree of detail, which is not warranted by the information contained in the set $\{S_l\}$ or by the nature of the physical situation. In practice, much smaller bases are often necessary in order to eliminate spurious oscillatory features from the potentials. The operation of the SVD algorithm, with adjustable SVD limit, stabilises the inversion and can, where appropriate, reduce the effective dimensionality of the inversion basis.

B. Single-energy inversion

In Ref. [8] we presented a test of $S \rightarrow V$ for deuterons scattering from the light nucleus ^{4}He in which there is very little absorption. Here we present a test for a much heavier nucleus, where there is substantial absorption, and demonstrate that a potential, very accurate almost to the nuclear centre, can be obtained by inversion. The test case studied was for a ^{58}Ni

---

[2]In our papers relating to spin 1/2 projectiles, the usual convention has been used.

target and deuterons at a laboratory energy of 56 MeV. The parameters found by Hatanaka *et al* [28] fitting angular distributions and the analyzing powers A_y and A_{yy} were used. A notable feature of the potential was that the imaginary T_R term was quite large, but the real T_R term was very small (a common but unexplained feature of deuteron optical potentials.) The spin-orbit component was real. The potential was parity independent as expected for this combination of target, projectile and energy. The energy and other characteristics of the reaction are such that there are 'many' active partial waves. 'Many' here means sufficient, even with $S_{l'l}^J$ for a single energy, to yield a precise reproduction of the potential.

The test was carried out as follows: one of the authors applied the optical model parameters of Hatanaka *et al* to the standard spin-1 scattering code DDTP [27], reading out the S-matrix onto a file. A second author, knowing only the target and the energy, then applied IMAGO to find the potential from these S-matrix elements. The inversion was carried out with a starting potential which contained only real and imaginary central potential components. These were guessed from general systematics without specific knowledge of Hatanaka's potential. Since with IMAGO there is complete freedom to choose the starting potential and inversion basis, it is worthwhile to test the inversion method starting with no more information about the potential than might be available in a 'for real' case.

When a converged solution was found, the potentials obtained were compared with the known potentials with results shown in Figure 1. The solid lines represent the 'target' potential, i.e. the potential from which the S-matrix was calculated using DDTP. The short dashes represent the potential found by inversion; it can be seen to reproduce the target potential very closely except very near to the nuclear centre in the case of the imaginary tensor component. We have not shown the real tensor component which was only a few percent of the imaginary component nearly everywhere. This small component was reproduced only qualitatively, as expected, since the absolute errors for the real and imaginary T_R components were similar in magnitude and comparable to the real T_R potential itself. In Figure 1, the dashed line represents the starting potential, zero for the spin-orbit and tensor components. The S-matrix elements for the target and inverted potentials are indistinguishable on a graph, corresponding to values of σ of roughly 10^{-3}.

This test shows that the inversion procedure has the capability of revealing quite fine details of the potential as would be required for the kind of applications, discussed in the introduction requiring the inversion of single energy S derived from theory. Such studies might establish, for example, the contribution of specific exchange terms or reaction couplings to the inter-nucleus potential.

C. Multi-energy inversion at very low energy

At low energies and for light target nuclei, very few partial waves are involved so that there will in general be insufficient information contained in the S-matrix elements for a single energy to yield a detailed and precise potential. The situation is even worse in cases where parity dependence must be assumed since this halves the information available for potential components of each parity. The problem can be ameliorated if S is available for more than one energy. If S is available over a narrow range of energies, then the algorithm can be made to yield to an energy independent potential; this is what we have earlier called

'mixed case' inversion (see Refs. [5,6] and first of Ref. [7]) and, in effect, the information from the energy derivative of S is exploited. In many cases, S_{lj} or $S_{l'l}^J$ are provided over a wide range of energies. In this case one should ideally consider the potential to be energy dependent and determine the energy dependence itself. This can be done within the framework of the parameterisations presented above.

An example of where the sets of S_{lj} or $S_{l'l}^J$ are too small to define the potential very closely is the $S \to V$ inversion situation embedded in the analysis of low energy, experimentally determined, multi-energy observables for d + alpha scattering. A first report was presented in Ref. [8]. The test we now describe is directly relevant and asks the following question: what properties of the potential can reliably be determined from very small sets of S?

The test was for deuterons scattering from ^{4}He with $S_{l'l}^J$ calculated from a known potential at 11 energies: 8, 8.5 ... 12.5, 13 MeV. The known potential was energy independent but parity dependent and was taken to be real. (The imaginary parts of empirical potentials are known to be small for d + ^{4}He at these energies.) The following terms were included: central Wigner, central Majorana, spin-orbit Wigner and separate even parity and odd parity T_R tensor potentials (the odd/even choice for T_R reflects what we believe [8] to be the case for the actual d + ^{4}He tensor force.) The central and spin-orbit terms are like those found in Ref. [8], and the very large even parity tensor term is based on that of Dubovichenko [29], see also [11].

The inversion was effectively 'mixed case' in the sense just described. The starting potential was zero in all components except for the Wigner real central and Wigner real spin-orbit terms. In keeping with the nature of this test, the very small inversion basis of Ref. [8] was used. This has two Gaussians only for each component except the central components for which there were three. The centres and widths of the Gaussians were not varied during the inversion.

The 'target' (known) and inverted potentials are shown in Figure 2, together with the starting potential required by the IP method. The starting potential is the dot dashed line, non-zero for two components only, and corresponding to $\sigma = 10.552$ where σ, defined in Section III B, is summed over the 11 energies. The inverted potential is shown as the dotted line, and the 'target' potential, from which $S_{l'l}^J$ was calculated, is the full line. We see that the qualitative features are reproduced although less well for the small components and near the nuclear centre. The value of σ for the potential shown in the dotted line was 0.135 which is reasonable for a low energy multi-energy case. For 10.5 MeV, this corresponds to $S_{l'l}^J$ for the target and inverted potentials being indistinguishable on a graph apart from one single term: the phase angle of the non-diagonal part of $S_{l'l}^J$ for higher partial waves for which, in any case, the magnitude $|S_{l'l}^J|$, $l \neq l'$, is very small. The tensor potential, having very different odd and even parity components, is as well reproduced as could be expected with the very small basis. Note that the starting potential for the inversion has zero tensor terms. From the matrix elements of T_R given in Section II B, we see that $l = 0$ partial waves are ineffective and hence we cannot expect to reproduce the tensor real term V_R at $r = 0$.

In summary: we found that the qualitative properties of the potential were reliably reproduced, particularly for the larger components. Thus, reliable statements about the general features of d + ^{4}He potentials can be made, but nothing can be asserted concerning non-central interactions for $r < 0.5$ fm.

V. INVERTING $S_{L'L}^J$ CALCULATED WITH A T_P TENSOR INTERACTION.

The inversion technique which we have described is limited to a tensor force of the T_R type. Since there exist processes which are expected to lead to T_P forces, the possibility must be faced that data analysed using the data-to-V extension of the inversion method, which is described in Section VI, will indeed involve a T_P tensor interaction. It is therefore relevant to ask, in the context of $S \to V$ inversion: can we invert $S_{l'l}^J$ calculated with a T_P tensor interaction with a potential which has only a T_R tensor interaction? If so, to what extent does inversion yield valid central and spin-orbit components?

There is further interest in knowing how well the general effects of a T_P interaction can be represented by a T_R potential. The properties and even existence of a T_P interaction have not yet been convincingly linked to experiment since the consequences of the two kinds of interaction are difficult to distinguish phenomenologically. This was discussed by Goddard [30] who compared $S_{l'l}^J$ and the observables calculated from a T_R interaction with the corresponding quantities calculated from a particular T_P interaction devised in such a way that, according to semi-classical arguments, it would be very similar in effect.

We study these questions by exploiting the equivalent pairs of tensor potentials introduced by Goddard. We first inverted $S_{l'l}^J$ for 30 MeV deuterons scattered from ^{56}Fe with a T_R potential and then inverted $S_{l'l}^J$ derived from the potential containing that T_P interaction which is 'equivalent' in Goddard's sense. The two potentials are given in Table 1 of Ref. [30].

The first part of the test showed that inversion of $S_{l'l}^J$ for a known T_R still works very well at about half the energy of the test described in Section IV B. The results were very similar: the T_R potential, which in this case is of a volume Woods-Saxon form with depth 5 MeV, is accurately reproduced even at the nuclear centre. The solid and (scarcely distinguishable) dashed lines in Figure 3 respectively represent Goddard's original potential and that found by inversion. The $S_{l'l}^J$ for the inverted potentials, including the non-diagonal terms, are indistinguishable on a graph from those for the original potentials.

The dotted lines in Figure 3, show the inversion for Goddard's T_P case. The non-tensor components are qualitatively well reproduced, the derived potentials having the appearance of the target potentials but with superimposed oscillations. This waviness is relatively more significant for the small components, the real central potential being reproduced to within a few percent for all r. The T_R interaction found by inversion is now surface peaked in form but of average depth comparable to that of the Woods-Saxon (which however had a local momentum dependence, see [30]). The *diagonal* $S_{l'l}^J$ for target and inverted potentials are graphically indistinguishable, as are arg $S_{l'l}^J$ for $l \neq l'$ for low values of J. However the non-diagonal S-matrix was not well reproduced for $J > 7$, for which partial waves the non-diagonal $|S_{l'l}^J|$ is very small. The value of σ was much higher than for the T_R case, i.e. 0.0294 compared with 0.00589.

The results presented graphically in Figure 3 can be quantified in terms of the volume integrals and rms radii for the central and spin-orbit components of the inverted potentials. For the T_R case, all of these quantities were reproduced to a few parts in a thousand with the (small) volume integral of the spin-orbit term being least accurate: the error was 0.7 %. The errors for the non-tensor components found when inverting Goddard's T_P potential were a few percent, the volume integral of the spin-orbit term again being least accurate with an error of 3.8 %.

Goddard also performed an identical comparison for the case of 13.0 MeV deuterons scattering from ^{46}Ti, and we repeated the test just described for this case. There is interest in doing this since the inversion algorithm applied to $S_{l'l}^J$ for a single energy is expected to fail at lower energies for reasons explained in Section IV C. However, we find that the results for 13 MeV deuterons on ^{46}Ti are essentially the same as for 30 MeV deuterons on ^{56}Fe for both $T_{\rm R}$ and $T_{\rm P}$ interactions. The form of the $T_{\rm R}$ potential representing the actual $T_{\rm P}$ component was essentially the same as that shown for 30 MeV in the bottom panel of Figure 3 and this similarity applies also to the deviations of the non-tensor terms. It therefore appears that we have found general properties of the $T_{\rm R}$ potential representing an actual $T_{\rm P}$ potential.

As a result of these tests, and noting that $T_{\rm P}$ interactions are not predicted to be particularly large, we conclude:

1. The existence of processes of the kind which give rise to a $T_{\rm P}$ component will not prevent this inversion procedure, which includes only $T_{\rm R}$ tensor interactions, from fitting $S_{l'l}^J$ and is unlikely to greatly falsify inversions of this kind, particularly with regard to the non-tensor components. IP spin-1 inversion as described here is thus not fatally undermined by the possible existence of $T_{\rm P}$ interactions. The effort needed to develop spin-1 inversion including $T_{\rm P}$ interactions require greater motivation than exists at present.

2. As Goddard suggested, almost all the effects of such a potential can be well represented by a $T_{\rm R}$ tensor interaction, although its relationship to the form of the $T_{\rm P}$ interaction is, as might be expected, more complicated than can be deduced from simple semi-classical arguments [30]. The phenomenological problem of establishing $T_{\rm P}$ interactions is still considerable.

VI. DATA TO POTENTIAL INVERSION FOR SPIN-1 PROJECTILES

In what follows, we first briefly indicate how $S \rightarrow V$ inversion is extended to (data) $\rightarrow V$ inversion for the uncoupled case, then indicate how this is extended to include coupling, as is required for spin-1 scattering.

A. Data to potential inversion for uncoupled situation

For clarity we suppress spin-related subscripts and begin by recasting Equation 7, using Equation 5, as [3,5,7]:

$$\frac{\partial S_l}{\partial \alpha_n^{(p)}} = \frac{\mathrm{i}m}{\hbar^2 k} \int_0^\infty (\psi_l(r))^2 v_n^{(p)}(r) \mathrm{d}r. \tag{19}$$

We now introduce a conventional χ^2 function:

$$\chi^2 = \sum_{k=1}^N \left(\frac{\sigma_k - \sigma_k^{\rm in}}{\Delta \sigma_k^{\rm in}} \right)^2 + \sum_n \sum_{k=1}^M \left(\frac{P_{kn} - P_{kn}^{\rm in}}{\Delta P_{kn}^{\rm in}} \right)^2 \tag{20}$$

where σ_k^{in} and P_{kn}^{in} are the input experimental values of cross sections and analyzing powers of type n (σ, $\text{i}T_{11}$, etc.) respectively. When fitting data for many energies at once, the index k indicates the angle and also the energy. Data re-normalising factors can be introduced as an additional contribution to Equation 20.

We must now expand χ^2 in terms of the $\alpha_n^{(p)}$. To do this we first linearize the calculated cross sections and analyzing powers, by expanding σ_k (and P_{kn}) about some current point $\{\alpha_n^{(p)}(i)\}$ (see Ref. [6]):

$$\sigma_k = \sigma_k(\alpha_n^{(p)}(i)) + \sum_{j,l} \left(\frac{\partial \sigma_k}{\partial S_l(E_k)} \frac{\partial S_l(E_k)}{\partial \alpha_n^{(p)}} \right)_{\alpha_n^{(p)}(i)} \Delta \alpha_n^{(p)}, \tag{21}$$

which applies at each iterative step $i = 0, 1, 2, \ldots$ and the correction (to be determined) for the n-th amplitude is $\Delta \alpha_n^{(p)} = \alpha_n^{(p)} - \alpha_n^{(p)}(i)$. Equivalent relations are applied for the P's.

Linear equations result from demanding that χ^2 is locally stationary with respect to variations in the potential coefficients $\alpha_n^{(p)}$, i.e. the derivatives of χ^2 with respect to the potential components $\alpha_n^{(p)}$ must vanish. Solving these linear equations is straightforward for any reasonable number of them and yields corrected values $\alpha_n^{(p)}(i)$. We then iterate the whole procedure, with wave-functions ψ_l in Equation 19 calculated using the corrected potentials from Equation 5, until convergence is reached. This algorithm almost always converges very rapidly, in general diverging only when highly inconsistent or erroneous data have been used or when the iterative process involves a very unsuitable starting point. Multi-energy $(\text{data}) \to V$ inversion is thus reduced to the solution of simultaneous equations in a series of iterative steps.

B. Generalisation to spin-1

Spin-1 $(\text{data}) \to V$ inversion is a natural generalisation of the above formalism with S_l replaced by $S_{l'l}^J$ and Eq. 19 replaced by the analogous form derived from Eq.8. It is shown in Ref. [8] that the system does indeed converge to a potential which fits the observables.

C. Evaluation of ambiguities for spin-1 $(\text{data}) \to V$ inversion

The tests of $(\text{data}) \to V$ inversion must reflect the way it will be applied; this is rather different than for $S \to V$ inversion. With the latter, one often has quite precise S calculated from a theory, and one then seeks quite precise and subtle properties of V, often relating to modifications of the theory. Inversion from measured observables is different because the data are generally far from complete and will contain statistical and, possibly, systematic errors. For this reason, we must be less ambitious concerning the details of the potential to be extracted. The test therefore ask the following question: for a situation with few active partial waves, how well-determined can we expect the potential to be?

As in $S \to V$ inversion, one must never attempt to establish details of the potential for which the input data carries no information. We must therefore apply the smallest possible inversion bases and accept approximate solutions. The penalty for excessive inversion basis dimensionality is the occurrence of spurious oscillatory features. In effect, at low energies

where the data is incomplete and featureless (reflecting the small number of partial waves), the goal of (data) $\rightarrow V$ inversion is to find the smoothest potential compatible with the data. IP inversion affords a level of control in this respect that is not possible with other inversion procedures.

The test we describe is for low energy $\vec{\mathrm{d}} + {}^4$He scattering. The results will be useful for interpreting previous fits to experimental data for this system. The following observables, σ, iT_{11}, T_{20}, T_{21} and T_{22}, were calculated at laboratory energies of 8, 9, 10, 11, 12 and 13 MeV using the same purely real, energy independent potential used in Section IV C. Apart perhaps from the extremely strong 'Dubovichenko-type' tensor interaction, very strongly peaked at $r = 0$, the general features of this potential are, we believe, similar to those of potentials which fit actual experimental data. This energy range is somewhat above the broad 2^+ resonances and the region of strong mixing between the 1^+ channels. The observables were evaluated for the six energies over a range of 20^0 to 170^0 CM, at intervals of one degree, and Gaussian noise was added as follows. For σ, 1% errors were imposed. For iT_{11}, the errors were 2% of the maximum magnitude and for the three tensor observables, 5% of the maximum magnitude.

We then applied (data) $\rightarrow V$ inversion to this multi-energy dataset, seeking a single energy independent potential. Following Section IV C and Ref. [8], the inversion bases for the Wigner and Majorana real central components consisted of three Gaussian functions. For the other components there were just two Gaussians. As in Section IV C, the starting potential was zero in all but the Wigner real central and Wigner real spin-orbit components. The results are shown in Figure 4 where we compare the known ('target') potential (solid lines), the chosen starting potential of the iterative method (dash-dotted lines, two components only), and two inverted potentials, shown as dashed and dotted lines. The dashed lines show the potential found after a first sequence of iterations and correspond to $\chi^2/F = 15.473$ where F, the number of degrees of freedom, was ~ 4500. This number arises since we seek simultaneous fits to five observables at six energies and 150 angles. The effective number of parameters is ~twelve. At this stage the reproduction of the larger components of the potential is fair, but the tensor terms are poor, with the even parity real tensor term being still almost zero. The corresponding fit to the model data is indicated by the set of dashed lines in Figure 5. The fit is of a quality which would be widely regarded as quite good when fitting experimental data, with only T_{22}, and perhaps T_{20} around 120 degrees, fitted poorly. The quality of fit to T_{21} is remarkable in view of the very poor reproduction of the tensor interaction.

A subsequent further set of iterations led to an almost perfect fit with $\chi^2/F = 1.2155$. Figure 4 shows that the potential, dotted, fits all parts of the potential except at quite small radii. In particular, the even parity real tensor is perfectly fitted for $r > 1$ but not fitted at all for $r < 1$. This is in accord with arguments given in Section IV C. As expected from the values of χ^2/F, the fits to the 10 MeV dataset, shown as dotted lines in Figure 5, are essentially perfect, being scarcely visible over the angular range of the artificial data. The same potential simultaneously fits the observables for the other five energies comparably well. We conclude that we could not expect to establish the various components of the potential to a higher degree of accuracy than shown in Figure 4 by fitting available experimental data. It is very salutary to see, in Figure 4, the profound change in the nature of the tensor interaction which follows the improvement of the fit revealed in Figure 5, comparing dashed

15

and dotted lines. The intermediate inversion, dashed lines in Figure 5, represents a fit of a quality which is often deemed acceptable when fitting experimental data. We note without further comment that the desirability of pursuing the best possible phenomenological fits is sometimes called into question.

It should be noted that the computing time required on a modern workstation to carry out the direct inversion of the data is very modest, and certainly much less than required to carry out a model independent optical model search, particularly one involving odd and even parity T_R components and about 4500 degrees of freedom.

In Ref. [9] we discussed the application of direct inversion of data as a method for phase shift analysis. It is therefore of interest to see the quality of fit to $S_{l'l}^J$ which corresponds to the two fits shown in Figure 5. The top three panels of Figure 6 show the phase shifts corresponding to the $l = J - 1$, $l = J$, $l = J + 1$ diagonal components of S, and the bottom panel presents half the argument of the non-diagonal S. The solid lines show the known potential, the dashed line is for the $\chi^2/N = 15.473$ fit and the solid line is for the $\chi^2/N = 1.2155$ fit. For two of the panels, the solid and dash-dot lines are nearly indistinguishable but they are clearly distinguishable in the other two, suggesting that there are limits to phase shift determination even when over some 4000 data are fitted with $\chi^2/N = 1.2155$.

We conclude that direct inversion is a practical, reliable and efficient means of determining a local potential which represents large, multi-energy datasets including tensor observables. The example presented here indicates the extent to which the results obtained by this method are meaningful at low energies where few partial waves are involved.

VII. SUMMARY AND CONCLUSIONS; SURVEY OF POSSIBLE APPLICATIONS

We have presented details of an inversion procedure which can be applied both to spin-1 projectiles scattering from a spin-0 target nucleus and to spin-$\frac{1}{2}$ plus spin-$\frac{1}{2}$ particle scattering. The non-diagonal $S_{l'l}^J$ yield a non-diagonal potential containing a tensor term. To our knowledge, this is the first time this has been achieved, and opens up the possibility of wide range of other inversion scenarios ranging from other channel spin-1 cases (such as p + ^{3}H scattering) to the inversion of S-sub-matrices of higher dimensionality. There are many other capabilities inherent in the underlying IP method: these include the possibility of inverting $S_{l'l}^J$ for several energies leading directly to an energy dependent potential, including bound state energies within the input data, and the ability to handle cases where parity dependence must be allowed for.

In this paper we have presented tests of IP $S \to V$ spin-1 inversion and evaluated its performance in 'difficult' cases. We showed that when there are sufficient active partial waves, the procedure yields very accurate potentials even quite near the nuclear centre. Where, on the other hand, there are few partial waves available to define each potential component, as is typical with light nuclei at low energies and where the potential is parity dependent, it is still possible to extract the qualitative features of a potential.

We also addressed the fact that the method is at present limited to T_R tensor interactions although it is quite probable that processes leading to T_P interactions are active. We showed

that $S_{l'l}^J$ arising from T_{P} interactions can be fitted quite well with a T_{R} tensor interaction and that, moreover, this does not lead to serious errors in the non-tensor components of the potential.

The IP inversion algorithm also forms the basis of a very efficient alternative way to find a multi-component local potential which fits elastic scattering data, particularly for multi-energy datasets. This is the direct (observable) $\rightarrow V$ inversion procedure in which the IP $S \rightarrow V$ inversion is embedded. This 'direct inversion' can be applied to spin-1 projectiles. We examined the ambiguity problems which arise in a 'difficult' (i.e. few partial waves, parity dependence) test case which is relevant to the evaluation of an analysis of low energy $\vec{\mathrm{d}} + {}^4$He scattering, the subject of a recent [8] and an extended future publication. Known potentials can be very well re-fitted, but it is clear that the non-central terms cannot be well established at the nuclear centre. In the course of performing this inversion test, it became apparent that fits of widely accepted quality lead to tensor potentials which have nothing in common with those determined by pursuing 'perfect fits'.

Finally, we remark that the method we have demonstrated here is certainly not limited in usefulness to deuteron scattering. It would certainly be worthwhile applying it the elastic scattering data for halo nuclei when these are of sufficiently substantial information content.

REFERENCES

[1] K.Chadan and P.C. Sabatier, 'Inverse Problems in Quantum Scattering Theory' 2nd Ed. (Springer-Verlag, New York, 1989)

[2] 'Inverse and algebraic quantum scattering theory', Ed. Apagyi *et al*, *Lecture Notes in Physics; Vol. 488* (Springer-Verlag, Berlin, 1997)

[3] R.S. Mackintosh and A.M. Kobos, Phys. Lett. **116B**, 95 (1982); A.A. Ioannides and R.S. Mackintosh, Nucl. Phys. **A438**, 354 (1985).

[4] V.I. Kukulin and V.N. Pomerantsev, Solution of inverse scattering problem with account of incompleteness and errors in input data. In: 'Microscopic methods in theory of few-body systems' (ed. A.M. Gorbatov), Kalinin, 1988, v.I, p.104.

[5] V.I. Kukulin, V.N. Pomerantsev and J. Horaček, Phys. Rev. **A 42**, 2719 (1990); V.I.Kukulin and V.N.Pomerantsev, Yad. Fiz. **51**, 376(1990) (English translation: Physics of Atomic Nuclei, **51**, 240 (1990)); V.I.Kukulin and V.N.Pomerantsev, Yad. Fiz. **60**, 1228(1997) (English translation: Physics of Atomic Nuclei, **60**, 1103 (1997)).

[6] V.I. Kukulin, V.N. Pomerantsev and S.B. Zuev, Yad. Fiz., **59**, 428 (1996); English translation: Physics of Atomic Nuclei, **59**, 403 (1996).

[7] S.G. Cooper and R.S. Mackintosh, Phys. Rev. **C 43**, 1001 (1991); Nucl. Phys. **A517**, 285 (1990); Nucl. Phys. **A576**, 308 (1994); Nucl. Phys. **A582**, 283 (1995); Phys. Rev. **C 54**, 3133 (1996)

[8] S.G. Cooper, V.I. Kukulin, R.S.Mackintosh and V.N. Pomerantsev, Phys. Rev. **C59**, 2361 (1999)

[9] S.G. Cooper, V.I. Kukulin, R.S. Mackintosh and E.V. Kuznetsova, Phys. Rev. **C58**, R31 (1998)

[10] G. R. Satchler, Direct Nuclear Reactions, (Clarendon Press, Oxford, 1983).

[11] V.I. Kukulin, V.N. Pomerantsev, S.G. Cooper, and S.B. Dubovichenko, Phys. Rev. **C 57**, 2462 (1998)

[12] J.M. Blatt and L.C. Biedenharn, Phys. Rev. **86**, 399 (1952)

[13] G.R. Satchler, Nucl. Phys. **21**, 116 (1960)

[14] A.P. Stamp, Nucl. Phys, **A159**, 399 (1970)

[15] A.A. Ioannides and R.C. Johnson, Phys. Rev. **C 17**, 1331 (1978)

[16] P.W. Keaton, Jr. and D.D. Armstrong, Phys. Rev. **C 8**, 1692 (1973)

[17] P. W. Keaton, Jr., E. Aufdembrink and L.R. Veeser, Los Alamos Scientific Laboratory Report No. LA-4379-MS, 1970 (unpublished)

[18] P. W. Keaton, Jr., Los Alamos Scientific Laboratory Report No. LA-6002, 1975 (unpublished)

[19] J. Raynal, Phys. Lett. **29B**, 93 (1969)

[20] R. Frick, H. Clement, G. Graw, P. Schiemenz and N. Seichert, Phys. Rev. Lett. **44**, 14 (1980)

[21] H. Clement, R. Frick, G. Graw, P. Schiemenz and N. Seichert, Z. Phys. A - Atoms and Nuclei, **314**, 49 (1983)

[22] R. Frick, H. Clement, G. Graw, P. Schiemenz, N. Seichert and Sun Tsu-Hsun, Z. Phys. A - Atoms and Nuclei **319**, 133 (1984)

[23] M. Matoba, M. Hyakutake and I. Kumabe, Phys. Rev. **C 32**, 1773 (1985)

[24] M. Ermer, H. Clement, P. Grabmayr, G.J. Wagner, L. Friedrich and E. Huttel, Phys. Lett. **188B**, 17 (1987)

[25] R.S. Mackintosh and A.M. Kobos, J. Phys. G: Nucl. Phys. **5**,359 (1979)

[26] S.G. Cooper, Program IMAGO, Open University Report OUPD9201 (revised 1998)

[27] R.P. Goddard, code DDTP, described and specified in University of Wisconsin Report, 1997. Our version was supplied by J.A. Tostevin.

[28] K. Hatanaka, K. Imai, S. Kobayashi, T. Matsusue, M. Nakamura, K. Nisimura, T. Noro, H. Sakamoto, H. Shimizu and J. Shirai, Nucl. Phys. **A 340**, 93 (1980)

[29] S.B. Dubovichenko, Physics of Atomic Nuclei, **61**, 162 (1988).

[30] R.P. Goddard, Nucl. Phys. **A291**, 13 (1977)

FIGURES

FIG. 1. Potential for deuterons scattering from ^{58}Ni at 56 MeV. From top, the real central, imaginary central, real spin-orbit and imaginary tensor terms. Solid lines represent the target (i.e. input) potential, dots the potential found by inversion and the dash-dot the starting potential of the inversion. The starting potential was zero for the real spin-orbit and the tensor terms. There was no imaginary spin-orbit potential; see text regarding the real tensor term.

FIG. 2. For deuterons scattering from ^{4}He for energies from $8 - 13$ MeV, the starting (dash-dot), inverted (dotted), and known, 'target', (solid) potentials. From the top, the potential components are: Wigner real central, Wigner real spin-orbit, even parity real T_R, Majorana real central and odd-parity real T_R.

FIG. 3. For deuterons scattering from ^{56}Fe at a laboratory energy of 30 MeV, comparing components (from top, the real central, imaginary central, real spin-orbit and real T_R) of the potential of Goddard (solid line) having a T_R term, the potential (dashes) found by inverting $S_{l'l}^J$ calculated from the solid line potential and the potential (dotted) found by inverting $S_{l'l}^J$ calculated from Goddard's 'equivalent' T_P-containing potential. The dashed and solid lines are only clearly distinguishable for the smallest, i.e. spin-orbit, component.

FIG. 4. For deuterons scattering from ^{4}He for energies from $8 - 13$ MeV, potentials found by direct inversion of artificial data incorporating Gaussian noise as described in the text. The starting potential, two components only, is shown as a dash-dotted line, the true ('target') potential is solid and the first stage ($\chi^2/N = 15.473$) and second stage ($\chi^2/N = 1.2155$) inversion potentials are shown dashed and dotted respectively.

FIG. 5. For deuterons scattering from ^{4}He for energies from $8 - 13$ MeV, the fits to the 10 MeV part of the six energy artificially generated datasets. The final fit with $\chi^2/N = 1.2155$ is the dotted line (visible in a few places only) and the intermediate fit with $\chi^2/N = 15.473$ is shown dashed.

FIG. 6. For deuterons scattering from ^{4}He for energies from $8 - 13$ MeV, fits to the diagonal (top three panels) and non-diagonal S-matrix. The solid curves correspond to the known potential, the S-matrix for the $\chi^2/N = 15.473$ fit is dashed and for the $\chi^2/N = 1.2155$ fit is dotted. As described in the text, the four panels are essentially the (real) phase shifts.
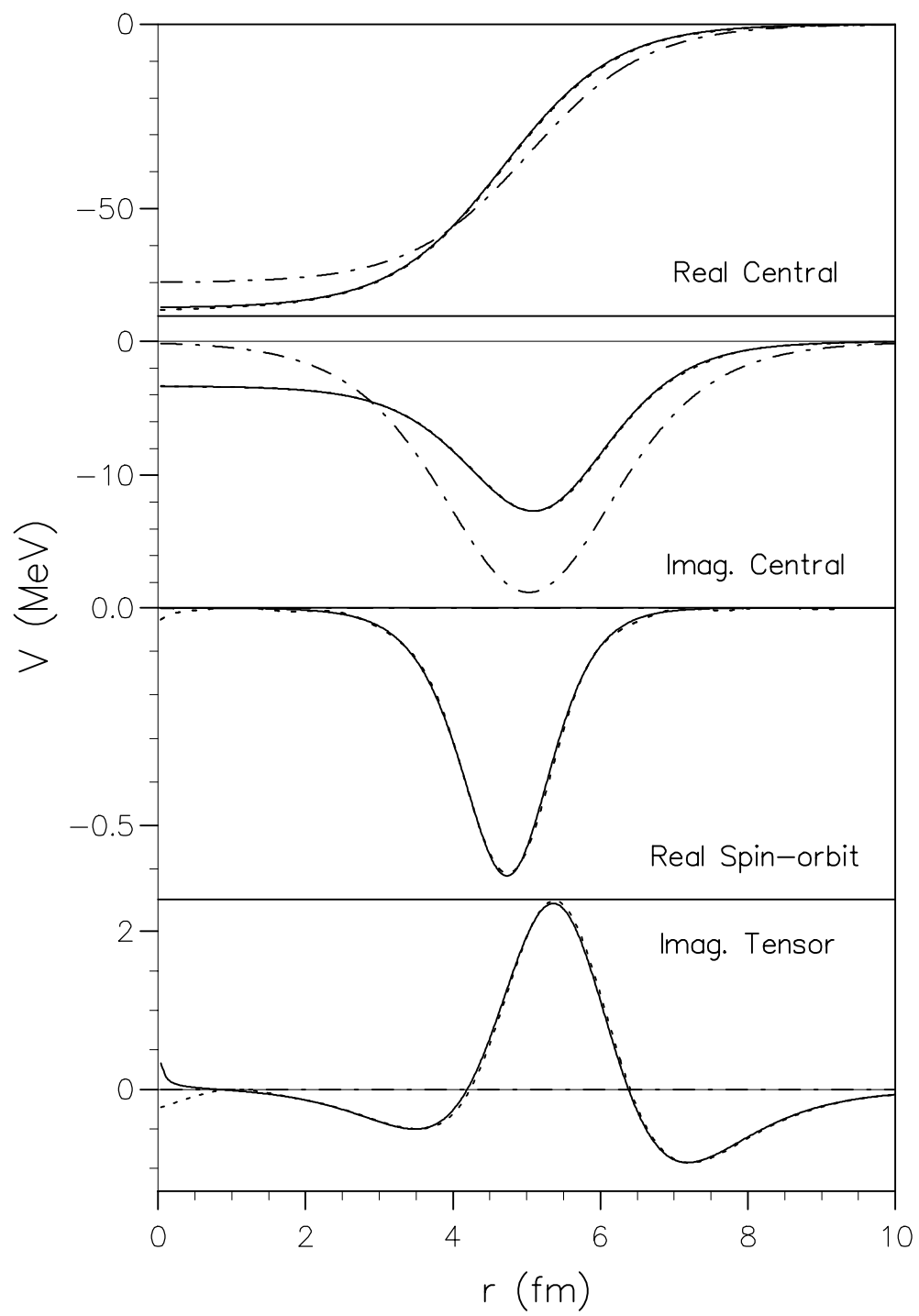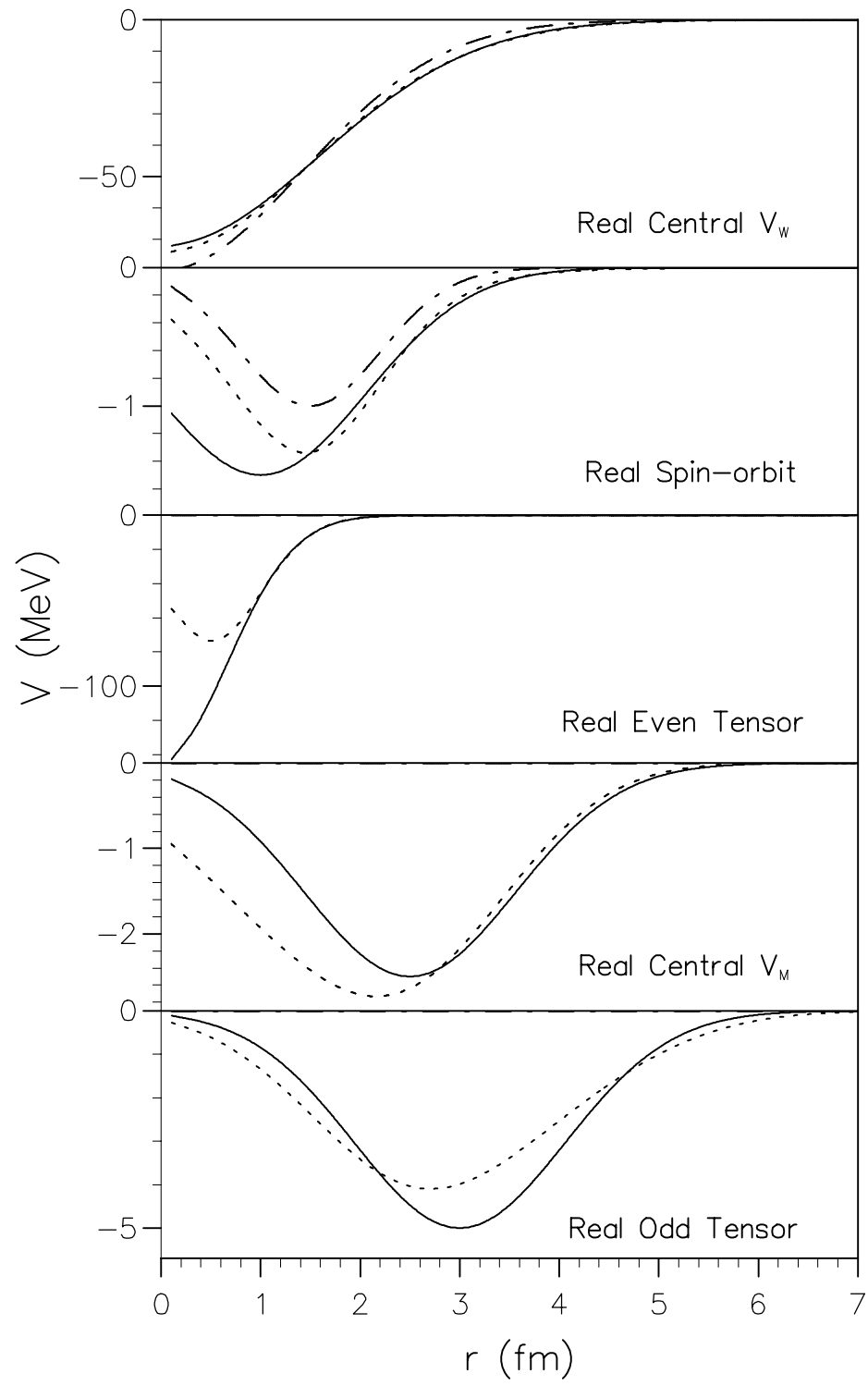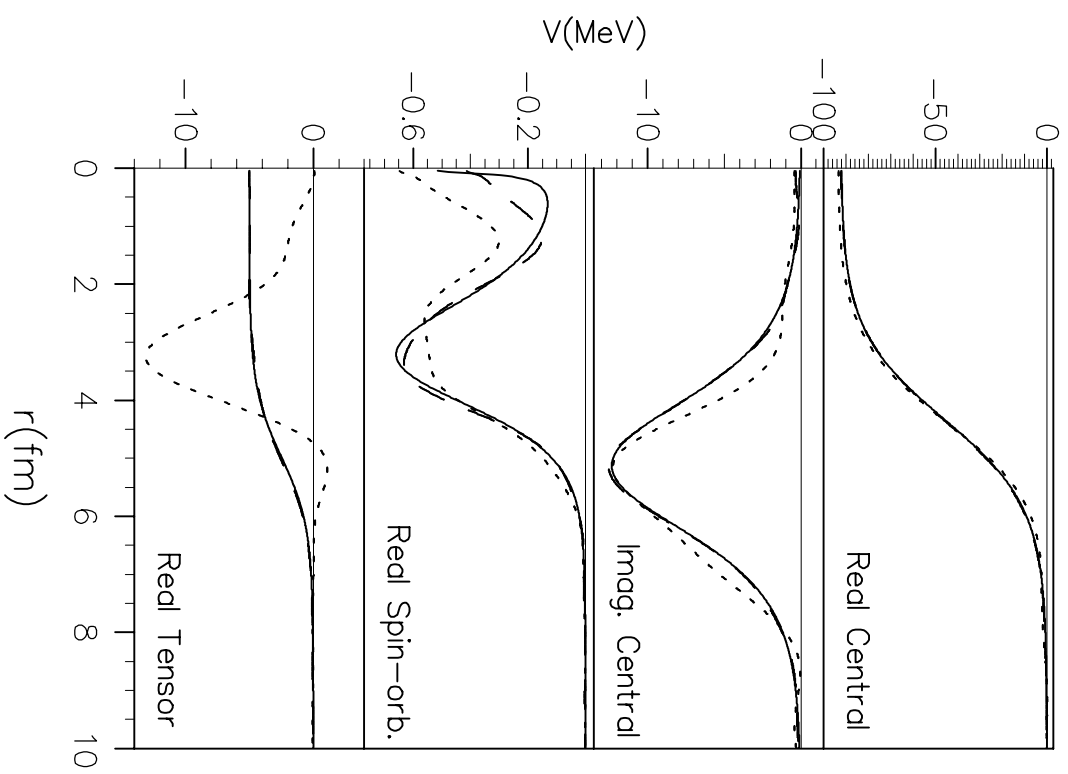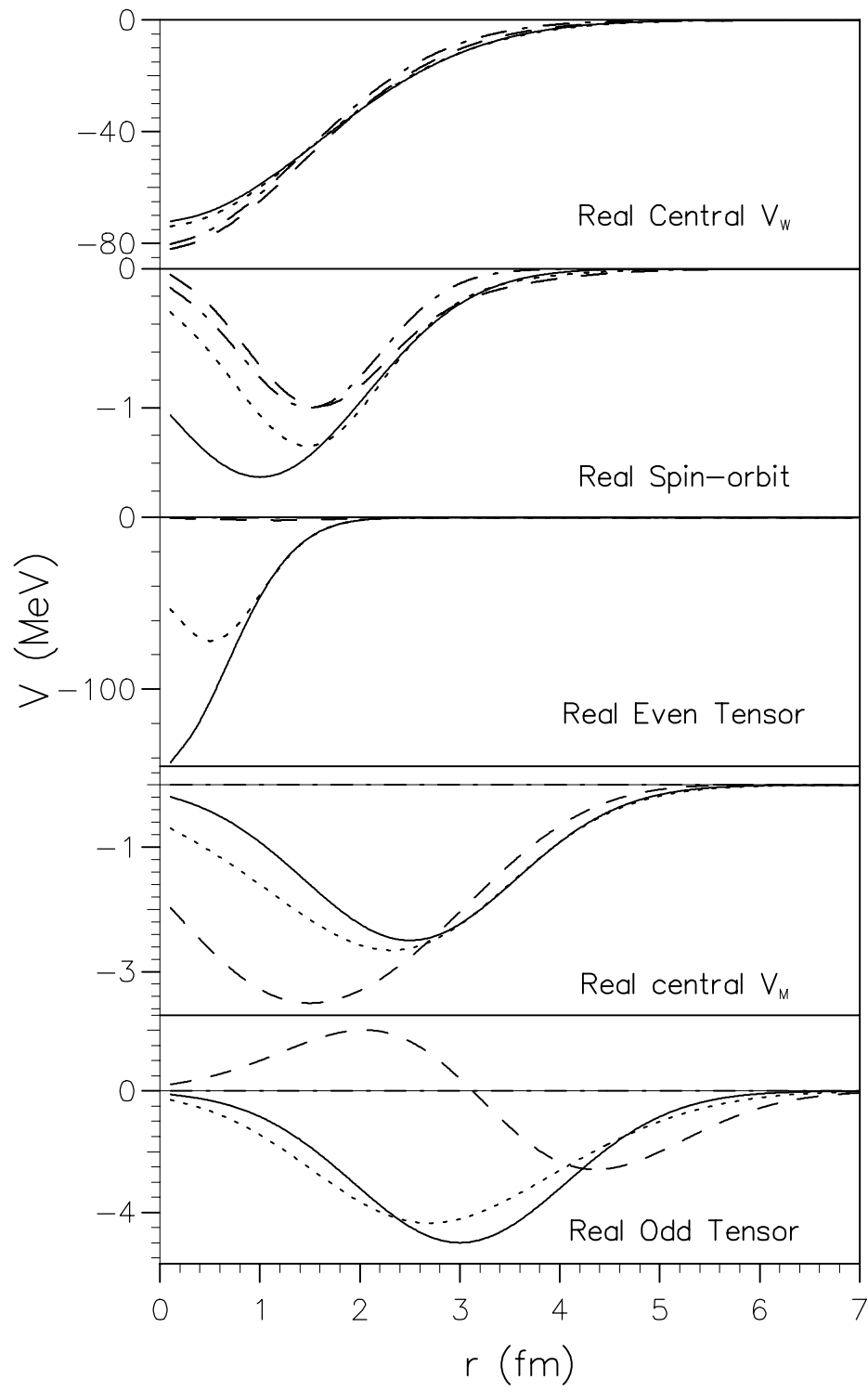
Fig. 1

Fig. 2

Fig. 3

Fig. 4

Real Central V_W

Real Spin-orbit

Real Even Tensor

Real central V_M

Real Odd Tensor

V (MeV)

r (fm)

Fig. 5

Fig. 6